



# Assessing various drought indicators in representing summer drought in boreal forests in Finland

Y. Gao<sup>1</sup>, T. Markkanen<sup>1</sup>, T. Thum<sup>1</sup>, M. Aurela<sup>1</sup>, A. Lohila<sup>1</sup>, I. Mammarella<sup>2</sup>, M. Kämäräinen<sup>1</sup>, S. Hagemann<sup>3</sup>, and T. Aalto<sup>1</sup>

<sup>1</sup>Finnish Meteorological Institute, P.O. Box 503, 00101 Helsinki, Finland

<sup>2</sup>University of Helsinki, Department of Physics, P.O. Box 48, 00014 Helsinki, Finland

<sup>3</sup>Max Planck Institute for Meteorology, Bundesstr. 53, 20146 Hamburg, Germany

Correspondence to: Y. Gao (yao.gao@fmi.fi)

Received: 23 July 2015 – Published in Hydrol. Earth Syst. Sci. Discuss.: 19 August 2015

Accepted: 10 December 2015 – Published: 18 January 2016

**Abstract.** Droughts can have an impact on forest functioning and production, and even lead to tree mortality. However, drought is an elusive phenomenon that is difficult to quantify and define universally. In this study, we assessed the performance of a set of indicators that have been used to describe drought conditions in the summer months (June, July, August) over a 30-year period (1981–2010) in Finland. Those indicators include the Standardized Precipitation Index (SPI), the Standardized Precipitation–Evapotranspiration Index (SPEI), the Soil Moisture Index (SMI), and the Soil Moisture Anomaly (SMA). Herein, regional soil moisture was produced by the land surface model JSBACH of the Max Planck Institute for Meteorology Earth System Model (MPI-ESM). Results show that the buffering effect of soil moisture and the associated soil moisture memory can impact on the onset and duration of drought as indicated by the SMI and SMA, while the SPI and SPEI are directly controlled by meteorological conditions.

In particular, we investigated whether the SMI, SMA and SPEI are able to indicate the Extreme Drought affecting Forest health (EDF), which we defined according to the extreme drought that caused severe forest damages in Finland in 2006. The EDF thresholds for the aforementioned indicators are suggested, based on the reported statistics of forest damages in Finland in 2006. SMI was found to be the best indicator in capturing the spatial extent of forest damage induced by the extreme drought in 2006. In addition, through the application of the EDF thresholds over the summer months of the 30-year study period, the SPEI and SMA tended to show more frequent EDF events and a higher frac-

tion of influenced area than SMI. This is because the SPEI and SMA are standardized indicators that show the degree of anomalies from statistical means over the aggregation period of climate conditions and soil moisture, respectively. However, in boreal forests in Finland, the high initial soil moisture or existence of peat often prevent the EDFs indicated by the SPEI and SMA to produce very low soil moisture that could be indicated as EDFs by the SMI. Therefore, we consider SMI is more appropriate for indicating EDFs in boreal forests. The selected EDF thresholds for those indicators could be calibrated when there are more forest health observation data available. Furthermore, in the context of future climate scenarios, assessments of EDF risks in northern areas should, in addition to climate data, rely on a land surface model capable of reliable prediction of soil moisture.

## 1 Introduction

Drought can be essentially defined as a prolonged and abnormal moisture deficiency (World Meteorological Organization, 2012). However, the cumulative nature of drought, the temporal and spatial variance during drought development, and the diverse systems that drought could have an impact on make drought difficult to quantify and define universally (Heim, 2002). The American Meteorological Society (1997) classifies drought into four categories: meteorological or climatological drought, agriculture or soil moisture drought, hydrological drought, and socio-economic drought. Drought is principally induced by a lack of precipitation. Furthermore,

high atmospheric water demand, due to warm temperatures, low relative humidity, and changes in other environmental variables, often coincides with the absence of precipitation (Hirschi et al., 2011). Through land–atmosphere interactions, prolonged meteorological drought can further exacerbate soil moisture drought, or even hydrological drought (Mishra and Singh, 2010; Tallaksen and Van Lanen, 2004).

A number of drought indicators have been developed in the past in order to quantify the characteristics of the different drought types and their potential impacts on diverse ecosystems and societies (Heim, 2002). The most prominent and widely used drought indicator is the Standardized Precipitation Index (SPI), which has been recommended as a standard drought indicator by the World Meteorological Organization (WMO) due to its flexibility for various timescales, simplicity in input parameters and calculation, as well as effectiveness in decision making (Sheffield and Wood, 2011; Hayes et al., 2011). The SPI was developed to provide a spatially and temporally invariant comparison of drought determined by precipitation at different timescales (McKee et al., 1993, 1995). The Standardized Precipitation–Evapotranspiration Index (SPEI) is developed based on the SPI, and, in addition to precipitation, also accounts for temperature impacts on drought (Vicente-Serrano et al., 2010). Soil moisture status has been explored through the Soil Moisture Anomaly (SMA) and Soil Moisture Index (SMI). The SMA has been adopted in the Coupled Model Intercomparison Project (CMIP) in order to study soil moisture drought in present and future projections in Global Circulation Models (GCMs) (Orlowsky and Seneviratne, 2013). The SMI (also referred to as Relative Extractable Water – REW) is often used to investigate soil water related plant physiology issues, as it can represent the relative plant available water in the root zone (Lagergren and Lindroth, 2002; Granier et al., 1999). Those drought indicators are globally applicable. However, only few studies have examined drought indicators against drought impact data in regional level (Blauhut et al., 2015). Drought studies in northern Europe are quite rare due to the low occurrence of drought. Nevertheless, a soil moisture index calculated with simulated soil moisture have been tested with the forest health observation data in Finland in Muukkonen et al. (2015).

Boreal forests have been recognized as a *tipping element* of the Earth system as they are highly sensitive to climate warming (Lenton et al., 2008). Bi et al. (2013) reported that satellite observations show substantial greening of Eurasia with climate warming; however, browning in the boreal region of Eurasia has also been found despite a much larger fraction of browning in the boreal region of North America due to less precipitation. Forest damage induced by drought is a cumulative effect and is closely linked to soil moisture (Granier et al., 2007). Reduction of tree transpiration at the stand level induced by the low soil moisture condition has been broadly observed in most tree species (Irvine et al., 1998; Bréda et al., 1993; Clenciala et al., 1998). In

recent years, micrometeorological flux networks with intensive ancillary data have greatly supported the investigation of the relationship between drought and carbon fluxes over diverse ecosystems (Grossiord et al., 2014; Krishnan et al., 2006; Welp et al., 2007; Law et al., 2002; Grünzweig et al., 2003). In general, those studies observed a growth reduction in forests as a consequence of drought. In addition to a reduction in forest productivity (Ciais et al., 2005; Granier et al., 2007), severe drought can lead to tree mortality in boreal forests (Allen et al., 2010; Peng et al., 2011). In spite of the frequency, duration and severity of droughts, drought-induced forest damages may be connected to specific soil and plant characteristics, such as soil texture and depth, exposure, species and their composition, and life stage (Muukkonen et al., 2015; Grossiord et al., 2014; Dale et al., 2001; Gimbel et al., 2015). Disturbance of boreal forests could give rise to further feedbacks to the global climate system, due to the complex interactions between boreal forests and the climate system via the control on energy, water, and carbon cycles (Bonan, 2008; Ma et al., 2012).

Soil moisture strongly regulates transpiration and photosynthesis for most terrestrial plants, consequently modulating water and energy cycles of the landscape, as well as biogeochemical cycles of the plants (Seneviratne et al., 2010; Bréda et al., 2006). Nevertheless, ground observed soil moisture is limited in time and space (Seneviratne et al., 2010). Regional analysis is necessary to fully capture the spatial heterogeneity of the impacts of drought on ecosystem functioning (Aalto et al., 2015). In recent years, a multi-decadal global soil moisture record that incorporates passive and active microwave satellite retrievals has become available (Liu et al., 2012). However, microwave remote sensing can only provide surface soil moisture in the upper centimetres of the soil. Land surface models (LSMs) are valuable tools to derive spatial maps of soil moisture in deeper soil layers, for instance, the root-zone soil moisture, which is of particular importance in many climate studies (Hain et al., 2011; Rebel et al., 2012; Seneviratne et al., 2010).

This study aims to improve our understanding of the properties of different drought indicators (including SPI, SPEI, SMA, and SMI), and assess their ability to indicate the Extreme Drought that affects Forest health (EDF) in boreal forests in Finland. The EDF is defined in this study according to the extreme drought in Finland in 2006, which caused visible impacts on forest appearance compared to normal years (Muukkonen et al., 2015). For the soil moisture drought indicators (SMA, SMI), regional soil moisture was simulated by the JSBACH LSM of the Max Planck Institute for Meteorology Earth System Model (MPI-ESM) with its five layer soil hydrology scheme. Thus, this study also aims to gain insights into the capability of the five layer soil hydrology scheme with its parameters in the JSBACH LSM to simulate soil moisture dynamics across Finland. The outcome of this study provides suggestions on the selection and interpreta-

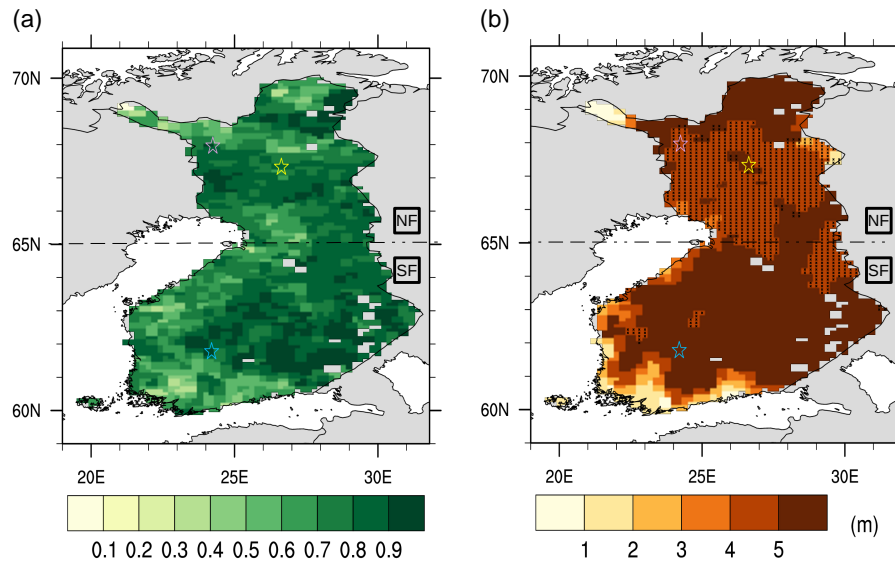


**Figure 1.** (a) The forest cover fraction over Finland in JSBACH derived according to Corine land cover 2006 data; (b) soil depth and the soil type (categorized as peatland and mineral soil) distributions in JSBACH over Finland (peatland area – dotted area; mineral soil area – area without dots). Northern (NF) and southern Finland (SF) are divided at the 65° N latitude. The location of the three ecosystem sites used in this study are marked as stars on the map (Blue–Hyytiälä; Yellow–Sodankylä; Pink–Kenttäröva). The uncovered grid boxes (grey cells) in Finland represent inland lakes.

tion of drought indicators for estimating EDF risks in boreal forests in future climate scenarios.

## 2 Study area and observation-based data sets

### 2.1 Study area

Our study area is focused on Finland (Fig. 1). Finland is a northern European country, situated between 60 and 70° N in the north-western part of the Eurasian continent, close to the North Atlantic Ocean.

The temperature of Finland is generally moderate, compared to many other places at the same latitudes (Tikkanen, 2005). This is because the westerly winds bring warm air masses from the North Atlantic Ocean in winter, while in summer they bring clouds that decrease the amount of incoming solar radiation. However, the continental high pressure system located over the Eurasian continent occasionally influences the climate causing warm and cold spells in summer and winter, respectively. The precipitation in Finland is influenced by the Scandinavian mountain range, which blocks large amounts of moisture that are transported from west to east. Both temperature and precipitation show spatial variations along a south to north gradient. The annual mean surface temperature is about 5–6 °C in the south of Finland and extends below –2 °C in the coldest area located in northern Lapland. Annual precipitation, averaged over the 1971–2000 period, is more than 700 mm in the south and less than 400 mm in the north (Aalto et al., 2013; Drebs et al., 2002).

In addition to mineral soils, a high areal fraction of peatland is typical for Finland, especially in the north of the country. Shallow soil areas accompanied with bare rocks are mostly located around the coastline in southern Finland and are also found in north-west Finland, which is a part of the Scandinavian mountain range.

Coniferous forest, including Scots pine and Norway spruce, is the dominant forest type in Finnish boreal forests (Finnish Statistical Yearbook of Forestry 2012, 2012). Broadleaved forest accounts for less than 10 % of the forest area. In total, 75 % of the total forest land area is located on mineral soils. In the past, large areas of unproductive peatlands have been drained to grow forests in Finland, as a result of the originally high proportion of pristine peatlands and timber production requirements (Päivänen and Hännell, 2012).

### 2.2 Meteorological and soil moisture data

The gridded meteorological data compiled by the Finnish Meteorological Institute (FMI gridded observational data) are interpolated products from stand meteorological observations in Finland (Aalto et al., 2013). In this study, daily FMI gridded observational data were used on a 0.2° longitude × 0.1° latitude grid for the period 1981–2010. These data comprise daily mean, minimum, and maximum temperatures, precipitation, relative humidity, and incoming short-wave radiation. In addition, the 10 m wind speed of ECWMF ERA-Interim reanalysis data (Simmons et al., 2007) was used to calculate the reference evapotranspiration ( $ET_0$ ) for

**Table 1.** Characteristics of the three micrometeorological sites. The plant functional types and the soil types in the JSBACH site simulations corresponding to observed tree species and soil types at the three sites are shown in brackets.

Site	Location	Period	Main tree specie	Soil type	Analysed measurement depth of soil moisture (cm)	Measurement technique for soil moisture	Reference
Hyytiälä	61°51' N, 24°18' E	1999– 2009	Scots Pine (Conifers)	Haplicpodzol (Mineral)	–5 to –23; –23 to –60	TDR	Vesala et al. (2005)
Sodankylä	67°21' N, 26°38' E	2001– 2008	Scots Pine (Conifers)	Sandy Podzol (Mineral)	–10, –20, –30 (averaged)	ThetaProbe	Thum et al. (2008)
Kenttäröva	67°59' N, 24°15' E	2008– 2010	Norway Spruce (Conifers)	Podzol (Mineral)	–10	ThetaProbe	Aurela et al. (2015)

SPEI from the Penman–Monteith equation (Allen et al., 1994).

In addition, meteorological and soil moisture data at three micrometeorological sites were used as meteorological forcing for site level simulations and for a comparison of modelled and observed soil moisture, respectively (Fig. 1; Table 1). Soil parameters derived from observations are only available for the Hyytiälä site (water content at saturation ( $\theta_{SAT}$ ) =  $0.50 \text{ m}^3 \text{ m}^{-3}$ , water content at field capacity ( $\theta_{FC}$ ) =  $0.30 \text{ m}^3 \text{ m}^{-3}$ , water content at wilting point ( $\theta_{WILT}$ ) =  $0.08 \text{ m}^3 \text{ m}^{-3}$ ). As explained in more detail below, we used the second layer of simulated soil moisture in the JSBACH soil profile (layer 2; 6.5–30 cm). Therefore, the observed soil moisture data were taken from existing measurement depths, which are consistent with the JSBACH layer 2 soil depth. For the Sodankylä site, an average of the measurements at soil depths –10, –20, and –30 cm was employed and for the Kenttäröva site, the measurement at –10 cm was used. The two levels in the Hyytiälä soil moisture measurement, –5 to –23 and –23 to –60 cm, were both used.

### 2.3 Forest health observation data

We adopted the yearly forest drought damage percentage in Finland from Muukkonen et al. (2015), who based their analysis on the forest health observation data from a pan-European monitoring programme ICP Forests (the International Co-operative Programme on the Assessment and Monitoring of Air Pollution Effects on Forests). The visual forest damage symptom inspections have been carried out by 10–12 trained observers during July–August since 2005, following internationally standardized methods (Eichorn et al., 2010) and national field guidelines (e.g. Lindgren et al., 2005). When a single sample tree in a site showed drought symptoms, it was recognized as a drought damage site. Therefore, uncertainties can rise from different personal interpretations and inappropriate time point of the visual inspections.

A 4-year (2005–2008) period of forest health observation data were analysed in Muukkonen et al. (2015). The summer of 2006 was extremely dry, and 24.4 % of the 603 forest health observation sites over entire Finland were affected, in comparison to 2–4 % damaged sites in a normal year. In southern Finland, 30 % of the observational sites showed drought symptoms.

## 3 Methods

### 3.1 JSBACH land surface modelling

JSBACH (Raddatz et al., 2007; Reick et al., 2013) is the LSM of the Max Planck Institute for Meteorology Earth System Model (MPI–ESM) (Stevens et al., 2013; Roeckner et al., 1996). It simulates energy, hydrology, and carbon fluxes within the soil–vegetation continuum and between the land surface system and the atmosphere. Diversity of vegetation is represented by plant functional types (PFTs). A set of properties are attributed to PFTs with respect to the various processes JSBACH is accounting for. For soil hydrology, a bucket scheme was originally used, in which the maximum water that can be stored in the soil moisture reservoir ( $W_{cap}$ ) corresponds to the root-zone water content (Hagemann, 2002). The bucket can be supplied from precipitation and snowmelt, but depleted through evapotranspiration (evaporation from the upper 10 cm of soil and plant transpiration from below), and lateral drainage. These processes are related to the amount of soil moisture in the bucket and are regulated by the Arno scheme, which separates rainfall and snowmelt into surface run-off and infiltration, and considers soil heterogeneity (Dümenil and Todini, 1992).

In order to more adequately simulate the soil hydrology, a five layer soil hydrology scheme has been newly introduced in JSBACH (Hagemann and Stacke, 2015). The five layer structure is defined with increasing layer thickness (0.065, 0.254, 0.913, 2.902, and 5.7 m) and reaches almost 10 m

depth below the surface. However, the soil depth to the bed rock, determines the active soil layers. Therefore, in the five layer soil hydrology scheme, the root zone is differentiated into several layers, and there could be soil layers below the root zone, which transport water upwards for transpiration when the root zone has dried out. Moreover, evaporation from bare soil can occur when the uppermost layer is wet, while the whole soil moisture bucket must be largely saturated in the bucket scheme. For a more detailed description of the five layer soil hydrology scheme in JSBACH and how it affects soil moisture memory, see Hagemann and Stacke (2015).

In this work, the regional JSBACH simulation was driven by the prescribed meteorological data (1980–2011) simulated by the regional climate model REMO (Jacob, 2001; Jacob and Podzun, 1997), whose temperature and precipitation biases were corrected with the FMI gridded observational data (Aalto et al., 2013). A quantile–quantile type bias correction algorithm was applied to daily mean temperature (Räisänen and Rätty, 2013), while daily cumulative precipitation was corrected using parametric quantile mapping (Rätty et al., 2014). The ECWMF ERA-Interim reanalysis (Dee et al., 2011) was used as lateral boundary data for the climate variables and as the initial values of surface climate variables for the REMO simulation. Both the regional JSBACH and REMO simulations were conducted in the Fennoscandian domain centred on Finland with a spatial resolution of  $0.167^\circ$  (15–20 km). The land cover distribution for REMO and the corresponding PDF distribution for JSBACH over this domain were derived from the more up-to-date and more precise Corine land cover 2006 data (European Environment Agency, 2007) rather than the standard GLCCD (US Geological Survey, 2001), which is important for simulating land–atmosphere interactions (Gao et al., 2015; Törmä et al., 2015). Finland is a country predominantly covered by forests. The forest cover fraction over Finland in JSBACH derived according to the Corine land cover 2006 data is shown in Fig. 1a. Also, an improved FAO (Food and Agriculture Organization of the United Nations) soil type distribution is adopted in the JSBACH LSM (FAO/UNESCO (1971–1981); see Hagemann and Stacke (2015), for details), while the soil depth distribution is derived from the soil type data set and FAO soil profile data (Dunne and Willmott, 1996) (Fig. 1b).

In addition, simulations were carried out for the three measurement sites with the observed local meteorological forcing. The characteristics of the sites together with the corresponding model settings are described in Table 1.

Prior to the actual regional and site level JSBACH simulations, long-term spin-ups were conducted to obtain equilibrium for the soil water and soil heat.

### 3.2 Drought indicators

A set of hydro-meteorological indicators were analysed. The SPI, SPEI, and SMA are standardized indicators that show the degree of anomalies to long-term means over the aggregation period, while SMI describes the instantaneous soil moisture status normalized with total soil moisture storage available to plants. In this study, daily SMI was used. The SPI, SPEI, and SMA were calculated with a 4-week (28 days) aggregation time frame, but they were updated every day with running inputs over the 30-year period. Both the 4-week aggregation time frame and 30-year study period are considered to be of sufficient duration climatologically under WMO guidelines (World Meteorological Organization, 2012). The SPI and SPEI were calculated using both the FMI gridded observational data set and the regional JSBACH forcing data described in the previous chapter, while SMA and SMI were computed with the layer 2 soil moisture from the regional JSBACH simulation. In addition, the SMIs were derived from site soil moisture observations, as well as from site JSBACH simulations. The layer 2 soil moisture from the JSBACH simulations was used, because the soil moisture in the shallower layer (layer 1) is highly sensitive to small changes in climatic variables, and the soil moisture dynamics in the deeper layers are excessively suppressed. Furthermore, the layer 2 is representative of the root zone in forest soils.

#### 3.2.1 Soil moisture index

The SMI is a measure of plant available soil water content relative to the maximum plant available water in the soil (Betts, 2004; Granier et al., 2007; Seneviratne et al., 2010). The soil water above field capacity cannot be retained, and produces gravitational drainage and usually flows laterally away. The soil water below the wilting point is strongly held by the soil matrix to such an extent that the plants are unable to overcome this suction to access the water (Hillel, 1998).

The SMI is calculated as follows:

$$\text{SMI} = (\theta - \theta_{\text{WILT}}) / (\theta_{\text{FC}} - \theta_{\text{WILT}}),$$

where  $\theta$  is the volumetric soil moisture [ $\text{m}_{\text{H}_2\text{O}}^3 \text{m}_{\text{soil}}^{-3}$ ],  $\theta_{\text{FC}}$  is the field capacity,  $\theta_{\text{WILT}}$  is the permanent wilting point.

Note that soil water content can exceed  $\theta_{\text{FC}}$  and reach water-holding capacity (i.e. saturation ratio) under certain circumstances. For those cases, the SMI is set to 1, indicating maximum plant available water.  $\theta_{\text{FC}}$  and  $\theta_{\text{WILT}}$  depend on soil types in this study, although  $\theta_{\text{WILT}}$  is also related to PFTs in some other studies. At Hyytiälä,  $\theta_{\text{SAT}}$  (saturation ratio) was used instead of  $\theta_{\text{FC}}$  to be consistent with the JSBACH soil hydrology where  $\theta_{\text{FC}}$  acts as a proxy for  $\theta_{\text{SAT}}$  on the large ESM grid scale (Hagemann and Stacke, 2015).

### 3.2.2 Soil moisture anomaly

The SMA is an index relevant to plant functioning (Burke and Brown, 2008). The SMA depicts the deviation of the soil moisture status in a certain period of a year to the soil moisture climatology over this period. It can be normalized by the standard deviation of the soil moisture in this respective period over all years, for direct comparison with the other standardized drought indicators, e.g. SPI, SPEI.

The SMA in this study is calculated following the method of Orłowsky and Seneviratne (2013):

$$\text{SMA} = (\bar{\theta} - \bar{\mu}) / \bar{\sigma},$$

where  $\bar{\theta}$  denotes the averaged volumetric soil moisture over a certain period in a year, while  $\bar{\mu}$  and  $\bar{\sigma}$  denote the mean and standard deviation of the volumetric soil moisture of this period over all the studied years.

### 3.2.3 Standardized precipitation index

The SPI inspects the amplitudes of precipitation anomalies over a desired period with respect to the long-term normal. The homogenized precipitation series is fitted into a normal distribution to define the relationship of probability to precipitation (Edwards and McKee, 1997). In this work, a Pearson type III distribution is adopted because it is more flexible and universal with its three parameters in fitting the sample data than the two parameter Gamma distribution (Guttman, 1994, 1999). The parameters of the Pearson type III distribution are fitted by the unbiased probability-weighted moments method. Typically, the timescales of SPI range from 1–24 months. The reduced precipitation under various durations can illustrate the impacts of drought on different water resources (Sivakumar et al., 2011). A time frame of less than 1 month is not recommended as the strong variability in weekly precipitation may lead to erratic behaviour in the SPI (Wu et al., 2007). However, the “moving window” of a minimum of 4 weeks with daily updating is acceptable (World Meteorological Organization, 2012). Furthermore, attention should be paid when interpreting the 1 month SPI to prevent misunderstanding. Large values in the 1 month SPI can be caused by relatively small departures from low mean precipitation (World Meteorological Organization, 2012).

The SPI is a probabilistic measure of the severity of a dry or wet event. An arbitrary drought classification with specific SPI thresholds was defined by McKee et al. (1993). Recently, an objective method based on percentiles from the United States Drought Monitor (USDM) has been recommended for defining location-specific drought thresholds (Quiring, 2009). For calculating SPI, we used the SPI function in R package SPEI version 1.6 (Beguería and Vicente-Serrano, 2013).

### 3.2.4 Standardized precipitation–evapotranspiration index

The SPEI is similar to SPI mathematically, but also accounts for the impact of temperature variability on drought through atmospheric water demand, in addition to the water supply from precipitation (Vicente-Serrano et al., 2010). The SPEI is based on a climatological surface water balance, which is calculated as the differences between precipitation and  $ET_0$ . In this work,  $ET_0$  was calculated according to the FAO-56 Penman–Monteith equation (Allen et al., 1994; Beguería and Vicente-Serrano, 2013), which is predominately a physical-based method and has been tested over a wide range of climates (Ventura et al., 1999; López-Urrea et al., 2006). The water balance time series is normalized by a log-logistic probability distribution and its parameter fitting is based on the unbiased probability-weighted moments method. For calculating SPEI, we used the SPEI function in R package SPEI version 1.6 (Beguería and Vicente-Serrano, 2013).

### 3.3 Assessment of JSBACH simulated soil moisture dynamics

In order to evaluate the ability of JSBACH simulated soil moisture to detect drought, the SMI series at the three study sites from the site and the regional (the model grids where the sites are located) JSBACH simulations were compared with the observed soil moisture data over the common data coverage periods (Table 1). SMI based on the Hyytiälä observational data was calculated with  $\theta_{\text{SAT}}$  and  $\theta_{\text{WILT}}$  values measured at the site. Due to the lack of measured soil parameters at the Sodankylä and Kenttäröva sites, the volumetric soil moisture measurements were directly used to examine the simulated soil moisture dynamics. An upper limit was set on the presented volumetric soil moisture to exclude abrupt and instantaneous peaks due to heavy snow melting or precipitation.

### 3.4 Intercomparison of drought indicators

The temporal and spatial coherency between the drought indicators was investigated at the regional level. The time correlations over our study period between the SPI calculated with the observational data set and the SPI calculated with the JSBACH forcing data were derived for the grid boxes in Finland. The same approach was adopted for the SPEIs. Moreover, the time correlations between the meteorological-based drought indicators (SPI, SPEI) calculated with the JSBACH forcing data and the soil moisture-based drought indicators (SMI, SMA) calculated with the JSBACH simulated soil moisture were derived for the grid boxes in Finland, as well as the time correlation between SMI and SMA. Furthermore, the spatial and temporal evolution of drought depicted by indicators was compared through time–latitude transections.

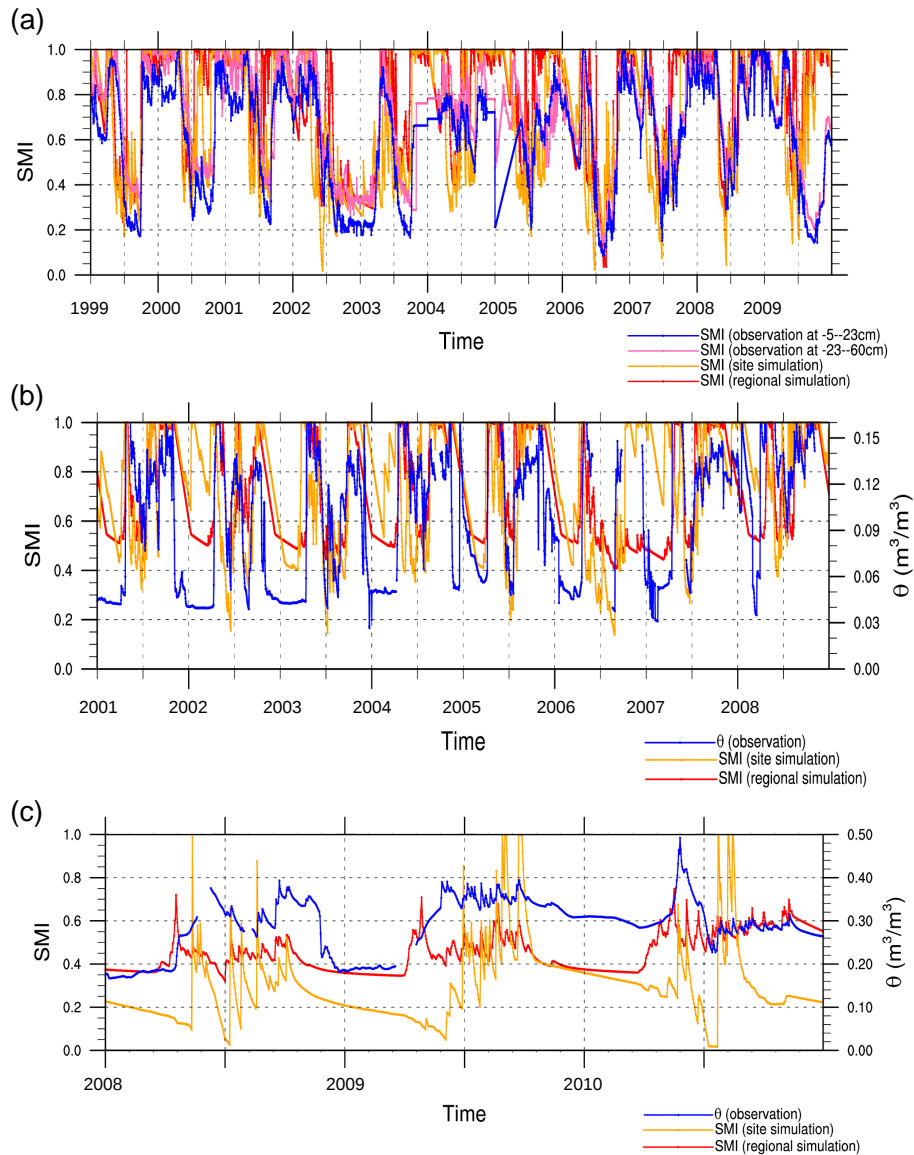


**Figure 2.** Soil moisture dynamics at the three micrometeorological sites: (a) Hyttiälä, (b) Sodankylä and (c) Kenttäröva, comparing results from regional (the model grid boxes where the sites are located) and site JSBACH simulations with observations. The volumetric soil moisture ( $\theta$ ) is shown for the Sodankylä and Kenttäröva sites.

### 3.5 Selection of EDF thresholds for indicators

According to the forest health observation data, we consider the 30 % forest damaged sites in southern Finland as the fraction of the area influenced by the severe drought in 2006, which is a reasonable assumption based on the dense and even distribution of observation sites over southern Finland. Based on this information, we utilized the cumulative area distributions of the SMI and SMA over southern Finland during the driest 28-day period of southern Finland in 2006 (i.e. in the case of SMI, this is the lowest 28-day-running mean value averaged over southern Finland) to derive their thresholds for this kind of extreme drought. Herein, as SMA

was calculated with 28-day-running means for soil moisture, the same time window was adopted for SMI to be consistent with SMA. The SPEI threshold for extreme drought is selected as 2 % of the SPEI data series, according to the recommended percentile classification (Quiring, 2009).

## 4 Results and discussion

### 4.1 Comparison of site soil moisture dynamics from JSBACH simulations with observations

In general, the timing of dry spells in summer in most of the years of the simulated soil moisture corresponded well with the observations at the three sites (Fig. 2). There was good agreement between the minimum values reached by the simulated and observed SMIs in summertime at Hyytiälä. The late summer of 2006 was noticeable as being extremely dry in the simulations and observations at Hyytiälä and Sodankylä. At Kenttäröva, the extent of the SMI was quite different in the regional and site JSBACH simulations. This was mainly because different soil types are prescribed for this site, which affects not only the soil hydrology but also the values of SMI. In the regional simulation, Kenttäröva was situated in a peat soil area, while in reality and in the site simulation the site is classified within a mineral soil area. The soil type in an individual grid for the regional simulation is homogeneous and defined according to the soil type with the highest coverage. The summer of 2010 was the driest among the three years at Kenttäröva according to the observation, and the timing of the driest period after mid-summer shown in the observations was successfully captured by the site simulation. Moreover, the soil at Kenttäröva was mostly unsaturated during those three years, even in the site simulations where it was realistically represented as a mineral soil. This is related to the small amount of precipitation during those years.

The diverse features of soil moisture among these sites in wintertime were captured by JSBACH. The soil tends to be saturated at Hyytiälä in winter, whereas at Sodankylä and Kenttäröva there is a winter recession period of soil moisture when the soil tends to dry out. At Hyytiälä, the difference is due to infiltration of snowmelt water during intermittent periods when air temperature is above 0 °C, while at Sodankylä and Kenttäröva, periods when the surface soil is frozen are more persistent and only percolation takes place then. The exceptionally low soil moisture during the winter 2003–2004 was also well simulated for Hyytiälä. This winter dry spell was caused by low rainfall in autumn 2003 and the relatively cold winter afterwards when there was not enough snowmelt water to recharge the deficit volume. This autumn-to-winter drought in 2003 at Hyytiälä was a rain to snow season drought (a precipitation deficit in the rainy season and at the beginning of the snow season) in combination with a cold snow season drought (see Van Loon and Van Lanen (2012) for the drought typology). The winter recession period of soil moisture at Kenttäröva is longer than that in Sodankylä, probably because Kenttäröva is located at higher latitudes. Large and obvious decreases in soil water immediately after the winter recession periods of soil moisture in 2008 and 2009 were shown by the site simulation, but not by the regional simulation. This is due to less precipita-

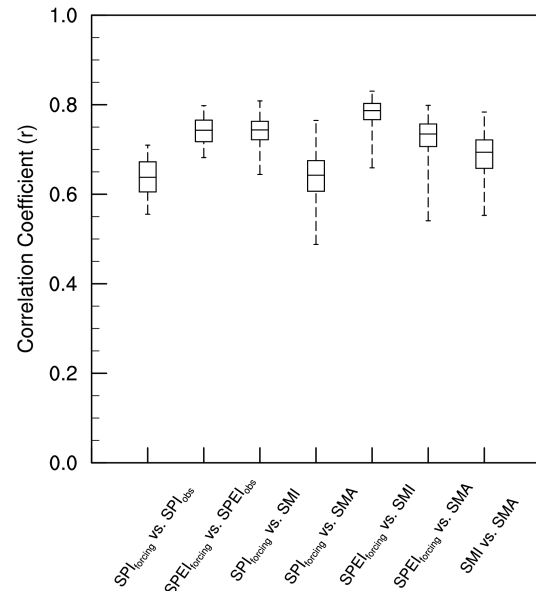


**Figure 3.** Percentiles of the time correlation coefficients across the grid boxes over Finland. The time correlations over the study period between the SPIs and SPEIs derived from the JSBACH forcing data and the observational data set (SPI<sub>forcing</sub> vs. SPI<sub>obs</sub>, SPEI<sub>forcing</sub> vs. SPEI<sub>obs</sub>), and the time correlations between SPI, SPEI calculated with the JSBACH forcing data and SMI, SMA calculated with the JSBACH simulated soil moisture (SPI<sub>forcing</sub> vs. SMI, SPI<sub>forcing</sub> vs. SMA, SPEI<sub>forcing</sub> vs. SMI, SPEI<sub>forcing</sub> vs. SMA), as well as the time correlation between SMI and SMA calculated with the JSBACH simulated soil moisture (SMI vs. SMA), are investigated. Dashed lines extend from 5th to 95th percentile of the correlation coefficients over Finland, boxes extend from 25th to 75th percentile and middle horizontal lines within each box are the medians. Those correlation coefficients are statistically significant ( $p < 0.01$ ).

tion during this period in the meteorological forcing data for the site simulation, in comparison to the regional simulation (data not shown). Moreover, the balance between water consumption through evapotranspiration and water gained from snowmelt was more negative in the site simulations. In general, the layer 2 soil moisture in the regional simulation for Kenttäröva captures the observed soil moisture dynamics at –10 cm depth better. However, a full evaluation would require observational data from several closely spaced soil layers.

Overall, the timing of summer dry spells and the winter characteristics of the observed soil moisture at the three sites were well captured by the simulated soil moisture, although the simulated soil moisture shows larger amplitudes and a faster response to changes in water inputs. The discrepancies in soil moisture between the site and the regional JSBACH simulations are mainly due to the differences in precipitation in summertime and in surface temperature during winter in the meteorological forcing data, as well as different soil types in specific locations. The latter is related to the difference in

scales between the regional grid and the site. Soil characteristics tend to be heterogeneous, so that the characteristics may vary on scales from a metre to a kilometre. While for modelling on the regional grid, effective soil characteristics are chosen that represent the average characteristics of a grid box.

#### 4.2 Intercomparison of drought indicators

The time correlations between the regional results of those drought indicators over our study period showed high correlation coefficients over Finland (Fig. 3). The medians of the time correlation coefficients over the whole of the country were greater than 0.6; with the 5 % percentiles also greater than 0.5, with the exception of the correlation coefficient between SMA and SPI. The agreement between SPEIs calculated with the JSBACH forcing data and the FMI gridded observational data set was better than that for SPIs. Furthermore, the soil moisture-based drought indicators revealed a better correspondence with SPEI than with SPI, which is reasonable as SPEI is based on the water balance. Therefore, in the following, we will focus on SPEI as the climatic driver indicator, and as there was a good correlation between the JSBACH forcing data and the FMI gridded observational data-based SPEIs, we restricted the data set by using the JSBACH forcing data-based SPEI, which was better related to the two soil moisture-based drought indicators from the model. Moreover, the correlation between SPEI and daily SMI was higher than that between SPEI and SMA. This is especially true for peatland areas while the correlations in mineral soil areas are more similar (see regional maps in the Supplement). This results from different soil moisture memory effects in those soil types.

From the time–latitude transections of the selected indicators (Fig. 4), the most exceptional dry years in our study period (e.g. 1994, 2006) can be distinguished, as well as the exceptionally wet years (e.g. 1981, 1998). Although there is generally a good correlation among all three indicators in capturing drought, there are differences among them in depicting drought durations and latitudinal extent at detailed locations and time. First, SPEI and SMA generally show more consistent patterns extending through a wider range of latitudes than SMI. Also, the buffering effect of soil moisture and the associated soil moisture memory can delay and extend dry or wet events as indicated by SMI and SMA, in comparison to those by the SPEI. For instance, the dry period in 1992 over southern Finland in SMI and SMA is longer than that in SPEI, and the wet period in the same year over northern Finland as indicated by SMA starts later in comparison to SPEI; however, this difference is not shown by SMI. Second, SMI exhibits a more distinct south–north gradient than the other two indicators. In particular, SMI describes more frequent droughts in the extreme southern parts of Finland. This is because the shallow soil in those areas is more sensitive to climate drivers. However, there is much less drought

indicated by SMI in the extreme northern part of the country (above 68° N). This could be due to the atmospheric water demand at the same SPEI drought level in the north is weaker than that in the south. In other words, the deviation of the multi-year mean value in precipitation surplus (precipitation – evapotranspiration) can lead to a higher change in SPEI values in the very north of Finland than in the south, as the variability of the climate in the north of Finland is lower. Third, SMI between latitudes 66 and 68° N shows an evident narrow range; i.e., the soil is not saturated or deeply dried out. This is due to the abundance of peatland areas with a larger soil moisture buffer than mineral soil areas.

SMI values vary within different ranges for the peatland and mineral soil areas in southern and northern Finland, whereas SMA and SPEI, as they are standardized indicators, show no differences regarding the soil type or location (Fig. 5). The regionally averaged SMI over the peatland areas mainly varies from 0.4 to 0.6 in both the south and north of Finland, while the SPEI averaged over the same area ranges between –2.0 and 2.0. SMI in the mineral soil shows larger variations compared to peat soil under the same climatic conditions. The SMI averaged over the mineral soil areas ranges between 0.1 and 1.0 in the south of Finland and 0.4 to 1.0 in the north of Finland. The higher values associated with the regionally averaged SMI in the north are due to less shallow soils and less meteorological drought in comparison to the south.

#### 4.3 EDFs indicated by drought indicators

Our results showed that the driest 28-day periods of southern Finland in 2006 were the same (from 20 July to 16 August) for SMI and SMA. The SMI and SMA thresholds for the EDF are 0.138 and –2.287, respectively (Fig. 6). Moreover, according to the recommended percentile classification (Quiring, 2009), the SPEI threshold for extreme drought, which is selected as 2 % of the SPEI data series, is –1.85 averaged over the grid boxes in Finland (–1.843 averaged over southern Finland). The averaged SPEI values over the EDF influenced areas in Finland depicted by SMI and SMA for the same period are –1.84 and –1.89, which are very close to the percentile-dependent SPEI threshold for extreme drought. This demonstrates that the degrees of EDF described by the derived SMI and SMA thresholds are consistent with the percentile-based threshold of extreme drought for SPEI, which is taken as the EDF threshold for SPEI.

Furthermore, we compared the regional distributions of the areas influenced by the 2006 EDF in the driest 28-day period indicated by SMI, SMA and SPEI (Fig. 7). The SMI showed that the EDF influenced areas were mainly located in southern Finland, whereas the SMA showed more EDF affected areas located in the middle to northern part of the country (mainly above 64° N). The EDF influenced areas presented by SMA in the north were mainly located in peatland areas, where the porosity of peat is much higher than

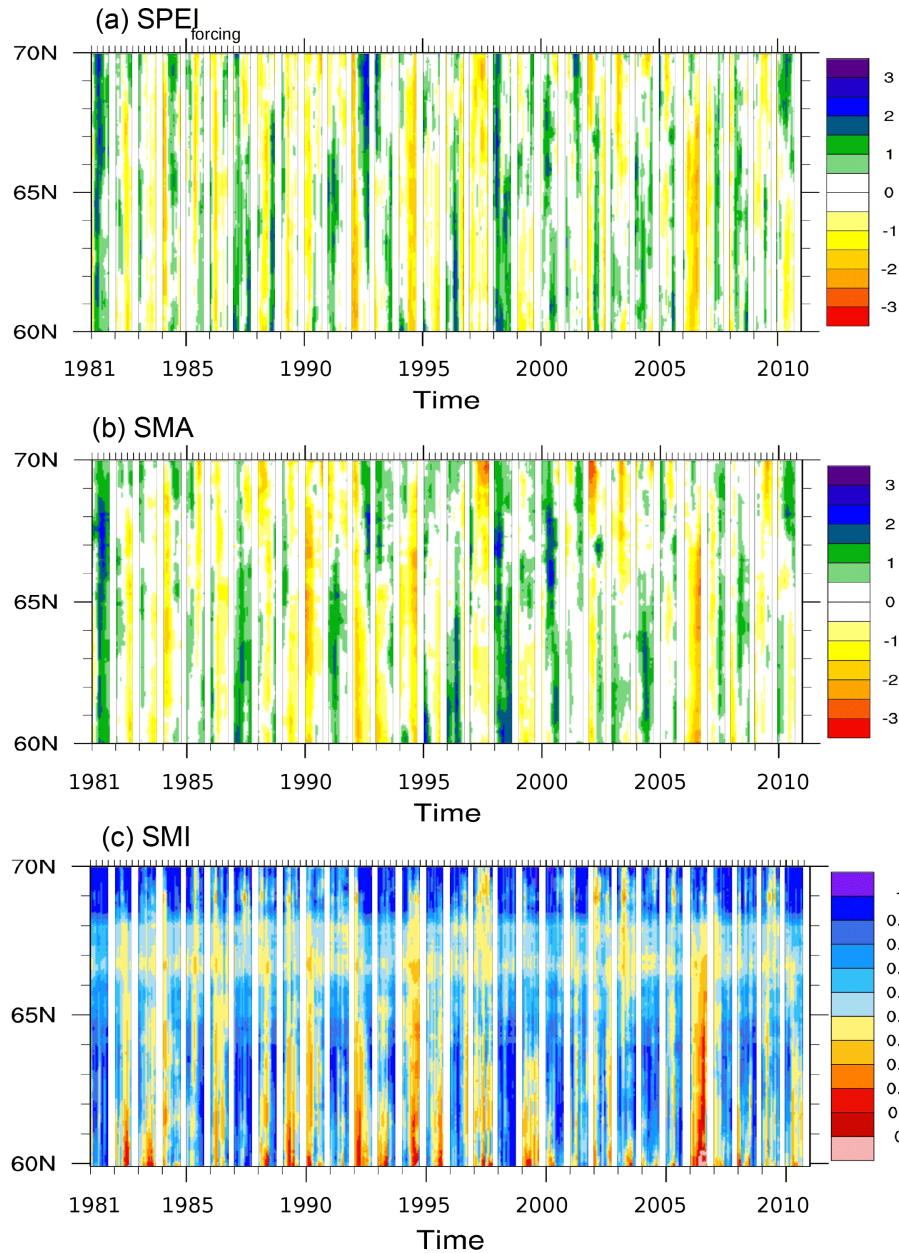


**Figure 4.** Latitude–time transections of (a) SPEI<sub>forcing</sub>, (b) SMA, and (c) SMI over Finland in the study period (the summer months (June, July, August) in 1981–2010).

that of mineral soils. Although there was a strong decrease in relative soil moisture with respect to the long-term mean value in those areas during this EDF event, the absolute soil moisture was not sufficiently low for those areas to be recognized as EDF in terms of SMI (Fig. 5). Moreover, the EDF influenced areas in the south-eastern part of Finland, as indicated by SMI, were not shown by SMA, although these areas comprise relatively low SMA values. This is because there were more EDF influenced areas indicated by SMA in the middle of Finland compared to SMI. Those areas took up a part of the 30% influenced area over the entire south-

ern Finland, which has been used for the selection of EDF thresholds by the cumulative area distributions. The areas impacted by EDF as indicated by SPEI, are widespread over Finland, complying with the climate conditions in this period. The extremely dry climate in northern Finland led to the EDF shown by SMA, but was not sufficiently intense for EDF to be captured by SMI. In southern Finland, the EDF areas of SMI generally agree with those of SPEI, except for the shallow soil area along the southern coastline and in the south-eastern part of the country (at 63° N). This more severe drought, which was indicated by SMI rather than by SPEI in

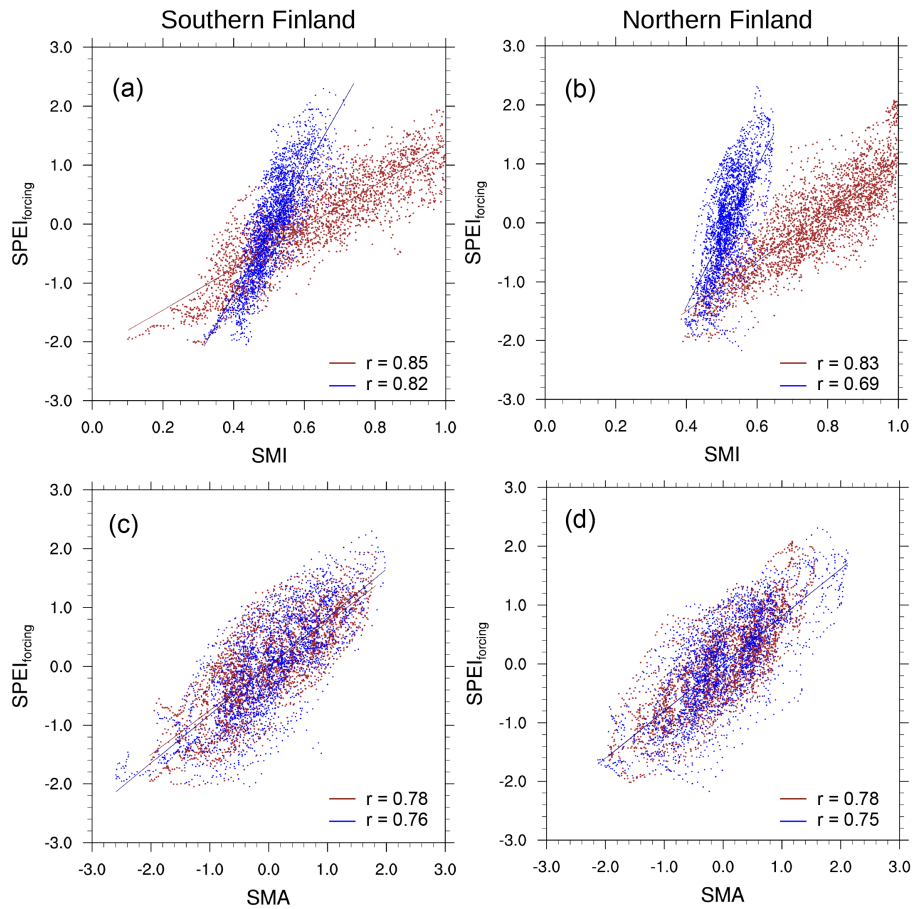


**Figure 5.** Time correlations over the study period between SPEI<sub>forcing</sub> and SMI (a, b), SPEI<sub>forcing</sub> and SMA (c, d) with the spatial means over the mineral soil areas (brown) and the peat soil areas (blue) in southern Finland (left column panels) and northern Finland (right column panels), respectively.

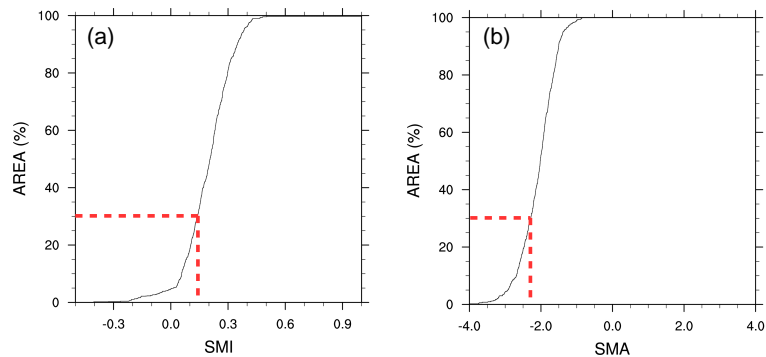


**Figure 6.** Cumulative area distribution of the (a) SMI and (b) SMA over southern Finland in the driest 28-day period of southern Finland in 2006 (i.e. the driest day of 28-day-running means of the regionally averaged SMI and SMA over southern Finland). The red dashed lines indicate the corresponding SMI and SMA values at which 30% of the area is affected by the Extreme Drought that affects Forest health (EDF).

the driest 28-day period, points to the vulnerability of shallow soil to climate variability. Also, it is worth noting that the EDF area in the driest 28-day period as indicated by the SMI, shows a similar spatial pattern to the locations of dam-

aged forest sites in the observation data, where few forest damaged sites are found in northern Finland.

A more comparative analysis of the ability of the three indicators to represent EDF under the derived thresholds was

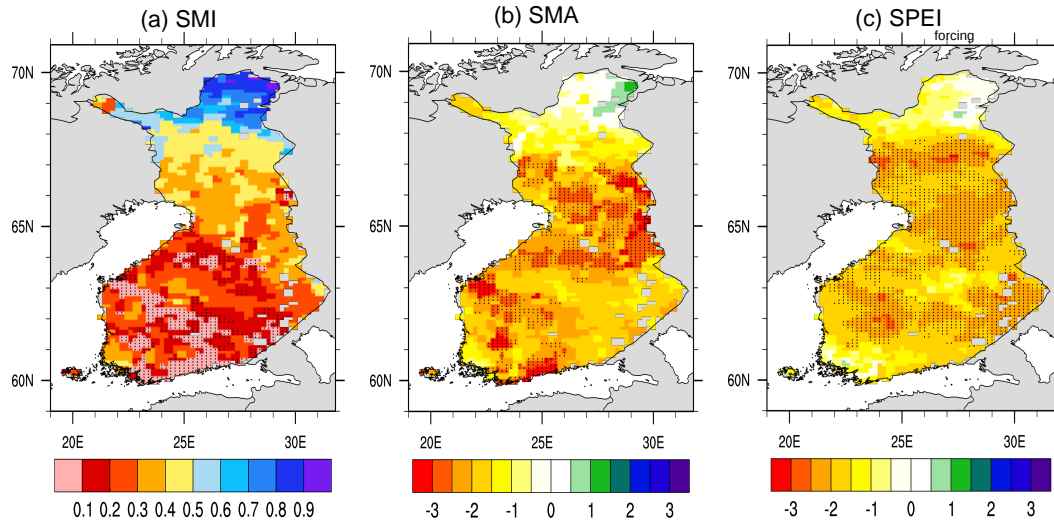


**Figure 7.** The (a) SMI, (b) SMA, and (c)  $SPEI_{forcing}$  in the driest 28-day period of southern Finland in 2006. The dotted areas are under the derived thresholds for EDF. The uncovered grid boxes (grey cells) in Finland represent inland lakes.

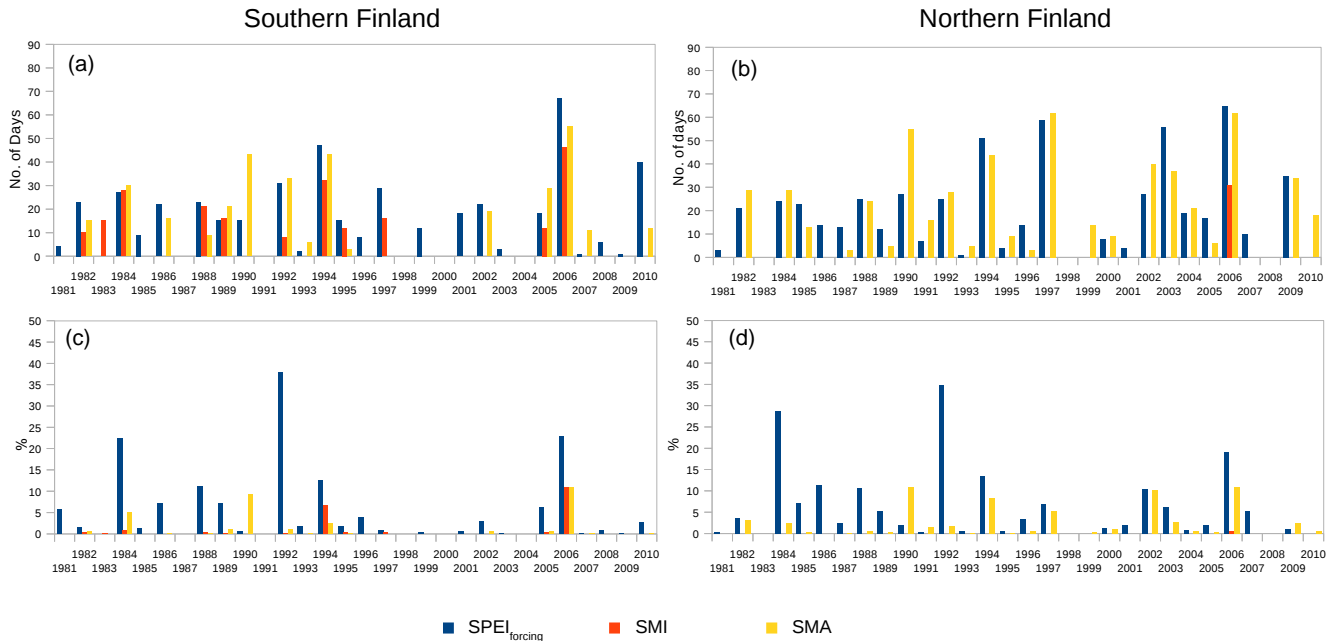


**Figure 8.** The summer drought periods (a, b) and the mean fractional areas affected by drought in these periods (c, d) induced by EDF events that are indicated by SMI, SMA, and  $SPEI_{forcing}$  for southern Finland (left column panels) and northern Finland (right column panels) in the study period (note that areas with shallow soil (soil depth < 3 m) are excluded).

conducted for the summer months of the 30-year study period (Fig. 8). As the shallow soil is quite sensitive to climate variation, areas with soil depths less than 3 m were excluded to eliminate the influence on drought period by sporadic drought episodes that would have exaggerated the number of drought days. In general, the drought periods (number of days) influenced by EDF show a better consistency among the three indicators than the mean fraction of affected areas.

In general, SMI shows less area under EDFs in both southern and northern Finland than the other two indicators. In particular, the only EDF indicated by SMI in the north was for 2006, but with only a small fractional area of around 1–2%. In the south, the SMI indicates EDF events in 1994 and 2006, with the mean influenced area larger than 5% and the period longer than 30 days. In 2006, the mean influenced areas indicated by the SMI and SMA are similar, as are the drought

periods. However, the SMA shows less mean influenced areas compared to SMI in 1994, which is related to the longer drought period indicated by SMA than SMI. The SPEI displays higher mean areas influenced by EDFs than the soil moisture drought indicators in all years, except 1990. The reason for this is that the EDF as indicated by SPEI in that year had already commenced before June, which is the first month of summer in our study. The SMA shows a prolonged effect in comparison to meteorological drought, which is not sufficiently strong to allow SMI to reach the EDF threshold due to the high initial soil moisture content.

Overall, the SMI is considered to be more capable in indicating EDFs because it directly reflects the plant available soil moisture. In boreal forests in Finland, EDFs indicated by SPEI and SMA often cannot lead to very low soil moisture that could be indicated as EDFs by SMI, due to the high initial soil moisture or presence of peat.

## 5 Summary and conclusions

In this study, we assessed the performance of several drought indicators (SPEI, SMA, and SMI) for their ability to represent the timing and spatial extent of droughts in Finland. The SPEI and SMA are standardized indicators that describe the degrees of anomalies over a period, whereas SMI is directly related to plant available water. Those standardized indicators were calculated with 28-days-running mean inputs, while SMI is calculated with daily soil moisture. The regional soil moisture is simulated by the land surface model JSBACH with its five layer soil hydrology scheme. The simulated soil moisture can generally capture the timing of dry spells in summer and winter characteristics of the observed soil moisture at the three observation sites in Finland, although inconsistencies exist in the rates of change and amplitudes of variations in soil moisture. The SPEI showed higher time correlation coefficients with the soil moisture-based drought indicators than SPI, as SPEI takes into account the surface water balance rather than precipitation only. Further inspections of the temporal and spatial variability of SPEI, SMA, and SMI revealed that, in general, the SPEI and SMA showed latitudinal-consistent patterns, whereas the SMI described more droughts for the south than the north of Finland. The vulnerable shallow soil area along the coastline in southern Finland and the peat soil area in northern Finland are drought-prone and drought-resistant areas, respectively, as indicated by SMI. Therefore, soil characteristics impact on SMI. In addition, soil moisture buffering effects and the associated soil moisture memory can delay and extend the drought as indicated by soil moisture-based drought indicators, in comparison to those by the SPEI.

Especially, we examined the effectiveness of SPEI, SMA, and SMI to capture the Extreme Drought affecting Forest Health (EDF). The SMI was found to be more capable in spatially representing the EDF in 2006. High discrepancies were

found among the indicated EDF periods and the mean fraction of affected areas by the three indicators for the summer months of the 30-year study period. The SPEI was the most sensitive drought indicator and showed the highest amount of EDFs with larger influenced areas, while the SMI showed much less EDF events than the other two indicators.

To conclude, we recommend to use SMI to indicate EDFs in boreal forest because it directly represents the plant available soil moisture, which is a synthesized result of the initial soil moisture content, soil properties, as well as climate conditions. Thus, a land surface model that produces reliable predictions of soil moisture is necessary when assessing EDF risks in boreal areas. To improve the accuracy of soil moisture-based drought indicators (especially SMI) calculated with LSM simulated soil moisture, high-quality soil type distribution and soil parameters data are essential. More sophisticated models are expected to improve simulated soil moisture; for instance, soil layers with different soil types along the soil profile, heterogeneity of soil types in a grid box and thorough consideration of the model formulations and parameters that regulate the rate of evapotranspiration, drainage and run-off. Furthermore, uncertainties associated with the drought indicators may originate from their input data (Naumann et al., 2014), therefore unbiased forcing data are of vital importance for the accurate simulation of soil moisture by a LSM (Maggioni et al., 2012).

The critical points of drought indicators leading to drought damages symptoms of forests are crucial for understanding climate impacts on forest ecosystems. In this study, the EDF thresholds for those indicators were selected only according to the statistics of the forest health observation in 2006. This might induce some uncertainties when they are used for future predictions of EDFs. The method for selecting EDF thresholds for drought indicators could be adopted and the EDF thresholds could be calibrated, when there are more observation data about forest damages induced by drought available. In addition, drought damage on different tree species could be studied. These would require more detailed information and a better monitoring at the forest observation sites. Moreover, satellite data could be explored to monitor the drought effects in boreal forests timely and across large spatial scale (Caccamo et al., 2011).

**The Supplement related to this article is available online at [doi:10.5194/hess-20-175-2016-supplement](https://doi.org/10.5194/hess-20-175-2016-supplement).**

*Acknowledgements.* We would like to thank the EMBRACE (EU 7th Framework Programme, Grant Agreement number 282672) and HENVI (Helsinki University Centre for Environment) projects for the financial support. We give our deepest appreciation to Pentti Pirinen from FMI for providing the observational data. The authors acknowledge MPI-MET, MPI-BGC, and CSC (Hamburg) for providing JSBACH and REMO models and assistance in their use, and also the MONIMET project

(LIFE12 ENV/FI/000409) for supporting the drought indicator study. This work was also supported by the Academy of Finland Center of Excellence (no. 272041), ICOS-Finland (no. 281255), and ICOS-ERIC (no. 281250) funded by Academy of Finland.

Edited by: A. Gelfan

## References

- Aalto, J., Pirinen, P., Heikkinen, J., and Venäläinen, A.: Spatial interpolation of monthly climate data for Finland: comparing the performance of kriging and generalized additive models, *Theor. Appl. Climatol.*, 112, 99–111, 2013.
- Aalto, T., Peltoniemi, M., Aurela, M., Böttcher, K., Gao, Y., Härkönen, S., Härmä, P., Kilkki, J., Kolari, P., Laurila, T., Lehtonen, A., Manninen, T., Markkanen, T., Mattila, O.-P., Metsämäki, S., Muukkonen, P., Mäkelä, A., Pulliainen, J., Susiluoto, J., Takala, M., Thum, T., Tupek, B., Törmä, M., and Ali, N. A.: Preface to the special issue on monitoring and modelling of carbon-balance-, water- and snow-related phenomena at northern latitudes, *Boreal Environ. Res.*, 20, 145–150, 2015.
- Allen, C. D., Macalady, A. K., Chenchouni, H., Bachelet, D., McDowell, N., Vennetier, M., Kitzberger, T., Rigling, A., Breshears, D. D., and Hogg, E. T.: A global overview of drought and heat-induced tree mortality reveals emerging climate change risks for forests, *Forest Ecol. Manage.*, 259, 660–684, 2010.
- Allen, R. G., Smith, M., Pereira, L. S., and Perrier, A.: An update for the calculation of reference evapotranspiration, *ICID Bulletin*, 43, 35–92, 1994.
- American Meteorological Society: Meteorological drought-policy statement, *B. Am. Meteorol. Soc.*, 78, 847–849, 1997.
- Aurela, M., Lohila, A., Tuovinen, J.-P., Hatakka, J., Penttilä, T., and Laurila, T.: Carbon dioxide and energy flux measurements in four northern-boreal ecosystems at Pallas, *Boreal Environ. Res.*, 20, 455–473, 2015.
- Betts, A. K.: Understanding Hydrometeorology Using Global Models, *B. Am. Meteorol. Soc.*, 85, 1673–1688, doi:10.1175/BAMS-85-11-1673, 2004.
- Beguiria, S. and Vicente-Serrano, S. M.: SPEI: Calculation of the standardised Precipitation–Evapotranspiration Index, R package version 1.6, R Foundation for Statistical Computing, Vienna, Austria, 2013.
- Bi, J., Xu, L., Samanta, A., Zhu, Z., and Myneni, R.: Divergent Arctic–Boreal Vegetation Changes between North America and Eurasia over the Past 30 Years, *Remote Sens.*, 5, 2093–2112, doi:10.3390/rs5052093, 2013.
- Blauhut, V., Gudmundsson, L., and Stahl, K.: Towards pan-European drought risk maps: quantifying the link between drought indices and reported drought impacts, *Environ. Res. Lett.*, 10, 014008, doi:10.1088/1748-9326/10/1/014008, 2015.
- Bonan, G. B.: Forests and Climate Change: Forcings, Feedbacks, and the Climate Benefits of Forests, *Science*, 320, 1444–1449, doi:10.1126/science.1155121, 2008.
- Bréda, N., Cochard, H., Dreyer, E., and Granier, A.: Water transfer in a mature oak stand (*Quercus petraea*): seasonal evolution and effects of a severe drought, *Can. J. Forest Res.*, 23, 1136–1143, doi:10.1139/x93-144, 1993.
- Bréda, N., Huc, R., Granier, A., and Dreyer, E.: Temperate forest trees and stands under severe drought: a review of ecophysiological responses, adaptation processes and long-term consequences, *Ann. For. Sci.*, 63, 625–644, 2006.
- Burke, E. J. and Brown, S. J.: Evaluating Uncertainties in the Projection of Future Drought, *J. Hydrometeorol.*, 9, 292–299, doi:10.1175/2007JHM929.1, 2008.
- Caccamo, G., Chisholm, L. A., Bradstock, R. A., and Puotinen, M. L.: Assessing the sensitivity of MODIS to monitor drought in high biomass ecosystems, *Remote Sens. Environ.*, 115, 2626–2639, doi:10.1016/j.rse.2011.05.018, 2011.
- Ciais, P., Reichstein, M., Viovy, N., Granier, A., Ogee, J., Allard, V., Aubinet, M., Buchmann, N., Bernhofer, C., Carrara, A., Chevalier, F., De Noblet, N., Friend, A. D., Friedlingstein, P., Grunwald, T., Heinesch, B., Keronen, P., Knohl, A., Krinner, G., Loustau, D., Manca, G., Matteucci, G., Miglietta, F., Ourcival, J. M., Papale, D., Pilegaard, K., Rambal, S., Seufert, G., Soussana, J. F., Sanz, M. J., Schulze, E. D., Vesala, T., and Valentini, R.: Europe-wide reduction in primary productivity caused by the heat and drought in 2003, *Nature*, 437, 529–533, 2005.
- Clenciala, E., Kucera, J., Ryan, M., G., and Lindroth, A.: Water flux in boreal forest during two hydrologically contrasting years; species specific regulation of canopy conductance and transpiration, *Ann. For. Sci.*, 55, 47–61, 1998.
- Dale, V. H., Joyce, L. A., McNulty, S., Neilson, R. P., Ayres, M. P., Flannigan, M. D., Hanson, P. J., Irland, L. C., Lugo, A. E., Peterson, C. J., Simberloff, D., Swanson, F. J., Stocks, B. J., and Michael Wotton, B.: Climate change and forest disturbances, *BioScience*, 51, 723–734, doi:10.1641/0006-3568(2001)051[0723:CCAFD]2.0.CO;2, 2001.
- Dee, D. P., Uppala, S. M., Simmons, A. J., Berrisford, P., Poli, P., Kobayashi, S., Andrae, U., Balmaseda, M. A., Balsamo, G., Bauer, P., Bechtold, P., Beljaars, A. C. M., van de Berg, L., Bidlot, J., Bormann, N., Delsol, C., Dragani, R., Fuentes, M., Geer, A. J., Haimberger, L., Healy, S. B., Hersbach, H., Hólm, E. V., Isaksen, I., Kållberg, P., Köhler, M., Matricardi, M., McNally, A. P., Monge-Sanz, B. M., Morcrette, J. J., Park, B. K., Peubey, C., de Rosnay, P., Tavolato, C., Thépaut, J. N., and Vitart, F.: The ERA-Interim reanalysis: configuration and performance of the data assimilation system, *Q. J. Roy. Meteorol. Soc.*, 137, 553–597, doi:10.1002/qj.828, 2011.
- Drebs, A., Nordlund, A., Karlsson, P., Helminen, J., and Rissanen, P.: Climatological statistics of Finland 1971–2000, in: Climatological Statistics of Finland 2001, Finnish Meteorological Institute, Helsinki, 2002.
- Dümenil, L. and Todini, E.: A rainfall–runoff scheme for use in the Hamburg climate model, in: Advances in Theoretical Hydrology – a Tribute to James Dooge, European Geophysical Society Series on Hydrological Sciences, edited by: O’Kane, J. P., Elsevier Science, Amsterdam, the Netherlands, 129–157, 1992.
- Dunne, K. and Willmott, C. J.: Global distribution of plant-extractable water capacity of soil, *Int. J. Climatol.*, 16, 841–859, 1996.
- Edwards, D. C. and McKee, T. B.: Characteristics of 20th century drought in the United States at multiple time scales. *Climatology Report 97-2*, Department of Atmospheric Science, Colorado State University, Fort Collins, Colorado, 1997.
- Eichhorn, J., Roskams, P., Ferretti, M., Mues, V., Szepesi, A., and Durrant, D.: Visual Assessment of Crown Condition and Damag-

- ing Agents Manual, Part IV in: Manual on methods and criteria for harmonized sampling, assessment, monitoring and analysis of the effects of air pollution on forests, UNECE ICP Forests Programme Co-ordinating Centre, Hamburg, 46 pp., 2010.
- European Environment Agency: CLC2006 technical guidelines, EEA Technical Report No. 17, Copenhagen, 2007.
- FAO/UNESCO: Soil Map of the World, UNESCO, Paris, 1971–1981.
- Finnish Statistical Yearbook of Forestry 2012, Finnish Forest Research Institute, Helsinki, Finland, 454 pp., 2012.
- Gao, Y., Weiher, S., Markkanen, T., Pietikäinen, J.-P., Gregow, H., Henttonen, H. M., Jacob, D., and Laaksonen, A.: Implementation of the CORINE land use classification in the regional climate model REMO, *Boreal Environ. Res.*, 20, 261–282, 2015.
- Gimbel, K. F., Felsmann, K., Baudis, M., Puhlmann, H., Gessler, A., Bruelheide, H., Kayler, Z., Ellerbrock, R. H., Ulrich, A., Welk, E., and Weiler, M.: Drought in forest understory ecosystems – a novel rainfall reduction experiment, *Biogeosciences*, 12, 961–975, doi:10.5194/bg-12-961-2015, 2015.
- Granier, A., Bréda, N., Biron, P., and Villette, S.: A lumped water balance model to evaluate duration and intensity of drought constraints in forest stands, *Ecol. Model.*, 116, 269–283, doi:10.1016/S0304-3800(98)00205-1, 1999.
- Granier, A., Reichstein, M., Bréda, N., Janssens, I. A., Falge, E., Ciais, P., Grünwald, T., Aubinet, M., Berbigier, P., Bernhofer, C., Buchmann, N., Facini, O., Grassi, G., Heinesch, B., Ilvesniemi, H., Keronen, P., Knohl, A., Köstner, B., Lagergren, F., Lindroth, A., Longdoz, B., Loustau, D., Mateus, J., Montagnani, L., Nys, C., Moors, E., Papale, D., Peiffer, M., Pilegaard, K., Pita, G., Pumpanen, J., Rambal, S., Rebmann, C., Rodrigues, A., Seufert, G., Tenhunen, J., Vesala, T., and Wang, Q.: Evidence for soil water control on carbon and water dynamics in European forests during the extremely dry year: 2003, *Agr. Forest Meteorol.*, 143, 123–145, doi:10.1016/j.agrformet.2006.12.004, 2007.
- Grossiord, C., Granier, A., Gessler, A., Jucker, T., and Bonal, D.: Does drought influence the relationship between biodiversity and ecosystem functioning in boreal forests?, *Ecosystems*, 17, 394–404, doi:10.1007/s10021-013-9729-1, 2014.
- Grünzweig, J. M., Lin, T., Rotenberg, E., Schwartz, A., and Yakir, D.: Carbon sequestration in arid-land forest, *Global Change Biol.*, 9, 791–799, doi:10.1046/j.1365-2486.2003.00612.x, 2003.
- Guttman, N. B.: On the sensitivity of sample L moments to sample size, *J. Climate*, 7, 1026–1029, doi:10.1175/1520-0442(1994)007<1026:OTSOSL>2.0.CO;2, 1994.
- Guttman, N. B.: Accepting the standardized precipitation index: a calculation algorithm, *J. Am. Water Resour. As.*, 35, 311–322, 1999.
- Hagemann, S.: An Improved Land Surface Parameter Dataset for Global and Regional Climate Models, Max Planck Institute for Meteorology, Hamburg, 2002.
- Hagemann, S. and Stacke, T.: Impact of the soil hydrology scheme on simulated soil moisture memory, *Clim. Dynam.*, 44, 1731–1750, doi:10.1007/s00382-014-2221-6, 2015.
- Hain, C. R., Crow, W. T., Mecikalski, J. R., Anderson, M. C., and Holmes, T.: An intercomparison of available soil moisture estimates from thermal infrared and passive microwave remote sensing and land surface modeling, *J. Geophys. Res.-Atmos.*, 116, D15107, doi:10.1029/2011JD015633, 2011.
- Hayes, M., Svoboda, M., Wall, N., and Widhalm, M.: The Lincoln declaration on drought indices: universal meteorological drought index recommended, *B. Am. Meteorol. Soc.*, 92, 485–488, doi:10.1175/2010BAMS3103.1, 2011.
- Heim, R. R.: A review of twentieth-century drought indices used in the United States, *B. Am. Meteorol. Soc.*, 83, 1149–1165, doi:10.1175/1520-0477(2002)083<1149:AROTDI>2.3.CO;2, 2002.
- Hillel, D.: *Environmental Soil Physics*, Academic Press, San Diego, 1998.
- Hirschi, M., Seneviratne, S. I., Alexandrov, V., Boberg, F., Boroneant, C., Christensen, O. B., Formayer, H., Orłowsky, B., and Stepanek, P.: Observational evidence for soil–moisture impact on hot extremes in southeastern Europe, *Nat. Geosci.*, 4, 17–21, doi:10.1038/ngeo1032, 2011.
- Irvine, J., Perks, M. P., Magnani, F., and Grace, J.: The response of *Pinus sylvestris* to drought: stomatal control of transpiration and hydraulic conductance, *Tree Physiol.*, 18, 393–402, doi:10.1093/treephys/18.6.393, 1998.
- Jacob, D.: A note to the simulation of the annual and inter-annual variability of the water budget over the Baltic Sea drainage basin, *Meteorol. Atmos. Phys.*, 77, 61–73, doi:10.1007/s007030170017, 2001.
- Jacob, D. and Podzun, R.: Sensitivity studies with the regional climate model REMO, *Meteorol. Atmos. Phys.*, 63, 119–129, doi:10.1007/BF01025368, 1997.
- Krishnan, P., Black, T. A., Grant, N. J., Barr, A. G., Hogg, E. T. H., Jassal, R. S., and Morgenstern, K.: Impact of changing soil moisture distribution on net ecosystem productivity of a boreal aspen forest during and following drought, *Agr. Forest Meteorol.*, 139, 208–223, 2006.
- Lagergren, F. and Lindroth, A.: Transpiration response to soil moisture in pine and spruce trees in Sweden, *Agr. Forest Meteorol.*, 112, 67–85, doi:10.1016/S0168-1923(02)00060-6, 2002.
- Law, B. E., Falge, E., Gu, L., Baldocchi, D. D., Bakwin, P., Berbigier, P., Davis, K., Dolman, A. J., Falk, M., Fuentes, J. D., Goldstein, A., Granier, A., Grelle, A., Hollinger, D., Janssens, I. A., Jarvis, P., Jensen, N. O., Katul, G., Mahli, Y., Matteucci, G., Meyers, T., Monson, R., Munger, W., Oechel, W., Olson, R., Pilegaard, K., Paw U, K. T., Thorgeirsson, H., Valentini, R., Verma, S., Vesala, T., Wilson, K., and Wofsy, S.: Environmental controls over carbon dioxide and water vapor exchange of terrestrial vegetation, *Agr. Forest Meteorol.*, 113, 97–120, doi:10.1016/S0168-1923(02)00104-1, 2002.
- Lenton, T. M., Held, H., Kriegler, E., Hall, J. W., Lucht, W., Rahmstorf, S., and Schellnhuber, H. J.: Tipping elements in the Earth's climate system, *P. Natl. Acad. Sci. USA*, 105, 1786–1793, doi:10.1073/pnas.0705414105, 2008.
- Lindgren, M., Nevalainen, S., Pouttu, A., Rantanen, H., and Salemaa, M.: Metsäpuiden elinvoimaisuuden arviointi, *Forest Focus/ICP Level 1*, Finnish Forest Research Institute, Helsinki, Finland, 56 pp., 2005.
- Liu, Y. Y., Dorigo, W. A., Parinussa, R. M., de Jeu, R. A. M., Wagner, W., McCabe, M. F., Evans, J. P., and van Dijk, A. I. J. M.: Trend-preserving blending of passive and active microwave soil moisture retrievals, *Remote Sens. Environ.*, 123, 280–297, doi:10.1016/j.rse.2012.03.014, 2012.

- López-Urrea, R., Olalla, F. M. d. S., Fabeiro, C., and Moratalla, A.: An evaluation of two hourly reference evapotranspiration equations for semiarid conditions, *Agr. Water Manage.*, 86, 277–282, doi:10.1016/j.agwat.2006.05.017, 2006.
- Ma, Z., Peng, C., Zhu, Q., Chen, H., Yu, G., Li, W., Zhou, X., Wang, W., and Zhang, W.: Regional drought-induced reduction in the biomass carbon sink of Canada's boreal forests, *P. Natl. Acad. Sci. USA*, 109, 2423–2427, doi:10.1073/pnas.1111576109, 2012.
- Maggioni, V., Anagnostou, E. N., and Reichle, R. H.: The impact of model and rainfall forcing errors on characterizing soil moisture uncertainty in land surface modeling, *Hydrol. Earth Syst. Sci.*, 16, 3499–3515, doi:10.5194/hess-16-3499-2012, 2012.
- McKee, T. B., Doeskin, N. J., and Kleist, J.: The relationship of drought frequency and duration to time scales, in: 8th Conference on Applied Climatology, Anaheim, California, 179–184, 1993.
- McKee, T. B., Doesken, N. J., and Kleist, J.: Drought monitoring with multiple time scales, in: Ninth Conference on Applied Climatology, Dallas, Texas, 233–236, 1995.
- Mishra, A. K. and Singh, V. P.: A review of drought concepts, *J. Hydrol.*, 391, 202–216, doi:10.1016/j.jhydrol.2010.07.012, 2010.
- Muukkonen, P., Nevalainen, S., Lindgren, M., and Peltoniemi, M.: Spatial Occurrence of Drought-Associated Damages in Finnish Boreal Forests: Results from Forest Condition Monitoring and GIS Analysis, *Boreal Environ. Res.*, 20, 172–180, 2015.
- Naumann, G., Dutra, E., Barbosa, P., Pappenberger, F., Wetterhall, F., and Vogt, J. V.: Comparison of drought indicators derived from multiple data sets over Africa, *Hydrol. Earth Syst. Sci.*, 18, 1625–1640, doi:10.5194/hess-18-1625-2014, 2014.
- Orlowsky, B. and Seneviratne, S. I.: Elusive drought: uncertainty in observed trends and short- and long-term CMIP5 projections, *Hydrol. Earth Syst. Sci.*, 17, 1765–1781, doi:10.5194/hess-17-1765-2013, 2013.
- Päivänen, J. and Hännel, B.: Peatland Ecology and Forestry: a Sound Approach, Department of Forest Ecology, University of Helsinki, Helsinki, 2012.
- Peng, C., Ma, Z., Lei, X., Zhu, Q., Chen, H., Wang, W., Liu, S., Li, W., Fang, X., and Zhou, X.: A drought-induced pervasive increase in tree mortality across Canada's boreal forests, *Nat. Clim. Change*, 1, 467–471, 2011.
- Quiring, S. M.: Developing objective operational definitions for monitoring drought, *J. Appl. Meteorol. Clim.*, 48, 1217–1229, doi:10.1175/2009JAMC2088.1, 2009.
- Raddatz, T. J., Reick, C. H., Knorr, W., Kattge, J., Roeckner, E., Schnur, R., Schnitzler, K. G., Wetzler, P., and Jungclaus, J.: Will the tropical land biosphere dominate the climate–carbon cycle feedback during the twenty-first century?, *Clim. Dynam.*, 29, 565–574, doi:10.1007/s00382-007-0247-8, 2007.
- Räisänen, J. and Räty, O.: Projections of daily mean temperature variability in the future: cross-validation tests with ENSEMBLES regional climate simulations, *Clim. Dynam.*, 41, 1553–1568, doi:10.1007/s00382-012-1515-9, 2013.
- Räty, O., Räisänen, J., and Ylhäisi, J.: Evaluation of delta change and bias correction methods for future daily precipitation: inter-model cross-validation using ENSEMBLES simulations, *Clim. Dynam.*, 42, 2287–2303, doi:10.1007/s00382-014-2130-8, 2014.
- Rebel, K. T., de Jeu, R. A. M., Ciais, P., Viovy, N., Piao, S. L., Kiely, G., and Dolman, A. J.: A global analysis of soil moisture derived from satellite observations and a land surface model, *Hydrol. Earth Syst. Sci.*, 16, 833–847, doi:10.5194/hess-16-833-2012, 2012.
- Reick, C. H., Raddatz, T., Brovkin, V., and Gayler, V.: Representation of natural and anthropogenic land cover change in MPI-ESM, *J. Adv. Model. Earth Syst.*, 5, 459–482, doi:10.1002/jame.20022, 2013.
- Roeckner, E., Arpe, K., Bengtsson, L., Christoph, M., Claussen, M., Dümenil, L., Esch, M., Gjogetta, M., Schlese, U., and Schultz-Weida, U.: The Atmospheric General Circulation Model ECHAM4: Model Description and Simulation of the Present-Day Climate, Max Planck Institute for Meteorology, Hamburg, 90 pp., 1996.
- Seneviratne, S. I., Corti, T., Davin, E. L., Hirschi, M., Jaeger, E. B., Lehner, I., Orlowsky, B., and Teuling, A. J.: Investigating soil moisture–climate interactions in a changing climate: a review, *Earth-Sci. Rev.*, 99, 125–161, doi:10.1016/j.earscirev.2010.02.004, 2010.
- Sheffield, J. and Wood, E. F.: Drought: Past Problems and Future Scenarios, Earthscan, London, UK and Washington, D.C., USA, 2011.
- Simmons, A., Uppala, S., Dee, D., and Kobayashi, S.: ERA-Interim: new ECMWF reanalysis products from 1989 onwards, *ECMWF Newsletter*, 110, 25–35, 2007.
- Sivakumar, M. V. K., Motha, R. P., Wilhite, D. A., and Wood, D. A.: Agricultural drought indices, in: Proceedings of the WMO/UNISDR Expert Group Meeting on Agricultural Drought Indices, 2–4 June 2010, Murcia, Spain, WMO/TD No. 1572; WAOB-2011, World Meteorological Organization, Geneva, Switzerland, AGM-11 197 pp., 2011.
- Stevens, B., Giorgetta, M., Esch, M., Mauritsen, T., Crueger, T., Rast, S., Salzmann, M., Schmidt, H., Bader, J., Block, K., Brokopf, R., Fast, I., Kinne, S., Kornblüeh, L., Lohmann, U., Pincus, R., Reichler, T., and Roeckner, E.: Atmospheric component of the MPI-M Earth System Model: ECHAM6, *J. Adv. Model. Earth Syst.*, 5, 146–172, doi:10.1002/jame.20015, 2013.
- Tallaksen, L. M. and Van Lanen, H. A. J.: Hydrological Drought: Processes and Estimation Methods for Streamflow and Groundwater, Elsevier Science B. V., the Netherlands, 2004.
- Thum, T., Aalto, T., Laurila, T., Aurela, M., Lindroth, A., and Vesala, T.: Assessing seasonality of biochemical CO<sub>2</sub> exchange model parameters from micrometeorological flux observations at boreal coniferous forest, *Biogeosciences*, 5, 1625–1639, doi:10.5194/bg-5-1625-2008, 2008.
- Tikkanen, M.: The Physical Geography of Fennoscandia, edited by: Seppälä, M., Oxford University Press, Oxford, 2005.
- Törmä, M., Markkanen, T., Hatunen, S., Härmä, P., Mattila, O.-P., and Arslan, A. N.: Assessment of land-cover data for land-surface modelling in regional climate studies, *Boreal Environ. Res.*, 20, 243–260, 2015.
- US Geological Survey: Global Land Cover Characteristics Data Base version 2.0, US Geological Survey, Reston, USA, 2001.
- Van Loon, A. F. and Van Lanen, H. A. J.: A process-based typology of hydrological drought, *Hydrol. Earth Syst. Sci.*, 16, 1915–1946, doi:10.5194/hess-16-1915-2012, 2012.
- Ventura, F., Spano, D., Duce, P., and Snyder, R. L.: An evaluation of common evapotranspiration equations, *Irrig. Sci.*, 18, 163–170, doi:10.1007/s002710050058, 1999.
- Vesala, T., Suni, T., Rannik, Ü., Keronen, P., Markkanen, T., Sevanto, S., Grönholm, T., Smolander, S., Kulmala, M., Ilves-

- niemi, H., Ojansuu, R., Uotila, A., Levula, J., Mäkelä, A., Pumpanen, J., Kolari, P., Kulmala, L., Altimir, N., Berninger, F., Nikinmaa, E., and Hari, P.: Effect of thinning on surface fluxes in a boreal forest, *Global Biogeochem. Cy.*, 19, GB2001, doi:10.1029/2004GB002316, 2005.
- Vicente-Serrano, S. M., Beguería, S., and López-Moreno, J. I.: A multiscalar drought index sensitive to global warming: the standardized precipitation evapotranspiration index, *J. Climate*, 23, 1696–1718, doi:10.1175/2009JCLI2909.1, 2010.
- Welp, L. R., Randerson, J. T., and Liu, H. P.: The sensitivity of carbon fluxes to spring warming and summer drought depends on plant functional type in boreal forest ecosystems, *Agr. Forest Meteorol.*, 147, 172–185, doi:10.1016/j.agrformet.2007.07.010, 2007.
- World Meteorological Organization: Standardized Precipitation Index User Guide, WMO-No. 1090, edited by: Svoboda, M., Hayes, M., and Wood, D., Geneva, Switzerland, 16 pp., 2012.
- Wu, H., Svoboda, M. D., Hayes, M. J., Wilhite, D. A., and Wen, F.: Appropriate application of the standardized precipitation index in arid locations and dry seasons, *Int. J. Climatol.*, 27, 65–79, doi:10.1002/joc.1371, 2007.